Planetary and Space Science 118 (2015) 8–13

Contents lists available at ScienceDirect

Planetary and Space Science

journal homepage: www.elsevier.com/locate/pss

A population of small refractory meteoroids in asteroidal orbits

M. Campbell-Brown *

University of Western Ontario, Department of Physics and Astronomy, London, ON, Canada N6A 3K7

ARTICLE INFO

Article history:
Received 8 January 2015
Received in revised form
2 March 2015
Accepted 25 March 2015
Available online 2 April 2015

Keywords:
Meteor
Interplanetary dust

ABSTRACT

More than 7000 two-station meteors observed with two different video systems, both parts of the Canadian Automated Meteor Observatory, have been analysed. The more sensitive (limiting magnitude +6.5) influx system shows a significant population of slow meteors with begin heights under 86 km, while the less sensitive (limiting magnitude +4) tracking system shows many more fast meteors ablating at high altitudes. The low, slow population has asteroidal orbits with low inclinations and moderate eccentricities, and radiants which are not, in general, associated with the sporadic sources. In spite of their low begin heights, which imply that they are strong and refractory, the meteors have early peaked light curves which are not predicted by classical ablation theory for non-fragmenting objects.

1. Introduction

The ablation height and speed distributions of meteors in the Earth's atmosphere are of great interest because of what they reveal about the origin and composition of asteroidal and cometary material striking the Earth.

The height at which a meteoroid begins to ablate depends on its speed, the angle at which it collides with the atmosphere, and its physical strength; in general, bodies moving faster, entering at shallower angles and with weaker or more volatile composition ablate higher. The effect of entry angle is the weakest effect: Štork et al. (2002) show the effect of speed and entry angle on begin and end heights; the speed has a strong effect, but the effect of zenith angle is only apparent in meteors with radiants less than 10° from the horizon. Begin heights are not strongly affected by the photometric mass, but there is a significant association between end height and mass (with more massive meteoroids having lower end heights).

Ceplecha (1967) introduced the k_B parameter to characterize the point at which the meteoroid had received enough energy to begin intensive ablation. He defined it as

$$k_B = \log_{10}\rho_B + 2.5\log_{10}(v_\infty) - 0.5\ \log_{10}\cos(z_R) \quad (1)$$

where ρ_B is the density of the atmosphere at the height at which the meteoroid becomes visible, in g cm^{-3}, v_∞ is the deceleration-corrected speed of the meteoroid, in cm s^{-1}, and z_R is the zenith distance of the radiant. k_B should depend only on the thermal properties of the meteoroid, notably the thermal conductivity, the specific heat, and the density. Later Ceplecha (1988) used the k_B parameter and orbital parameters to divide meteoroids into five strength categories, corresponding to asteroidal, ordinary chondrites, carbonaceous chondritic material, and strong and weak cometary material. The boundaries between the categories must be adjusted with detector sensitivity, since the beginning height of a meteor is higher in more sensitive systems (Kikwaya et al., 2011).

Among the populations of meteors which can be identified based on begin height and speed, there is an interesting population with low speeds and begin heights which are low even among slow meteors.

Borovička et al. (2005) examined spectra and orbits of 97 meteors, mostly between +3 and −1 magnitude. Of these, 14 were identified as iron-rich, with spectra almost exclusively composed of iron lines. This group had low speeds and low begin heights, and all of them had asteroidal orbits, with Tisserand parameters with respect to Jupiter of more than 3; all but two had inclinations of 10° or less. Most were very faint: all but one were fainter than +2.5 and most peaked between +3 and +4. All of the meteors had light curves which peaked in the early part of the trajectory, contrary to what would be expected from classical single body theory, and most had sudden onsets, which started with the brightest part of the trail. The authors speculated that this might involve a transition from solid iron to liquid.

A few high-density meteoroids were also found in a small survey of very faint (down to +7 magnitude) meteors in Kikwaya et al. (2009). Six meteors with complete light curves from very sensitive, small field intensified cameras were carefully modelled, and three of them had densities over 4000 kg m^{-3}. The three meteors had speeds of 30 km s^{-1} or less, ablated at heights under 100 km, and had light curves which peaked early in the trajectory; they were also among the faintest of the sample.

* Tel.: +1 5196612111.
E-mail address: margaret.campbell@uwo.ca

http://dx.doi.org/10.1016/j.pss.2015.03.022
0032-0633/

2. Observations

The Canadian Automated Meteor Observatory (CAMO) consists of two stations separated by approximately 45 km; Elginfield, at 43.193°N, 81.316°W, and Tavistock, at 43.265°N, 80.772°W. Each site houses three intensified video cameras; one pair of wide and narrow field cameras which incorporate computer-controlled mirrors to track meteors in the sky (the tracking system), and one camera referred to as the influx system.

The influx system uses a Gen III ITT NiteCam image intensifier (18 mm until November 2011 (Elginfield) and July 2012 (Tavistock), and 25 mm thereafter), coupled to a Cooke pco.1200 camera, with a 50 mm f/0.95 objective lens. The camera records video at 20 frames per second, 14 bit optical depth; the progressively scanned images were 1K × 1K before the intensifier change, and 1600 × 1200 pixels after. It has a 20° field of view, and an effective limiting meteor magnitude of $+6.5^M$. The main purpose of the system is monitoring meteoroid flux.

The tracking system has two 18 mm Gen III NiteCam image intensifiers coupled to ImperX VGA-120 cameras. The wide field system has a 25 mm f/0.85 lens and a field of view of 28°; the narrow field system has a 545 mm f/11 telescope as an objective and a field of view of 1.5°. It is not used in this study. The wide field system runs at 80 progressive frames per second, 640 × 480 pixels, with an optical depth of 12 bits. It has an effective limiting magnitude of $+4^M$, and is used to automatically detect meteors for tracking with the narrow field system. The system is described in detail in Weryk et al. (2013).

CAMO has been recording data since June of 2009. The influx system, which was the first system to become operational, has recorded 5092 two-station meteors until 2012, while the tracking system recorded just over 4000 two station meteors between June 2010 and October 2014.

Meteors recorded in the wide field tracking camera are detected and reduced in realtime using the ASGARD software package (Weryk et al., 2008). The threshold for detection is set relatively high, since only brighter meteors can reliably be tracked. The influx system uses MeteorScan (Gural, 1997) to detect meteors after night's data have been recorded; the process has the thresholds set relatively low, and false alarms are mostly removed by comparing the two systems to find common meteors; only two station meteors are saved. After detection, meteors from the influx system are reduced manually using the METAL software package (Weryk and Brown, 2012).

Since we are analysing for this work only those meteors which begin and end in the field of view, the relative area of overlap of each system as a function of height is of interest. The tracking system has a peak overlap area at 90 km; the overlap area is half as large at 65 km and 143 km, and there is no overlap above 165 km. The influx system has a peak overlap area at 120 km, and falls to half that at 82 km, and a quarter at 72 km. The relative overlap area is still 60% of the maximum at 180 km, the highest height for which it has been computed.

3. Height and speed distributions

Rather than plotting histograms of observed speeds and beginning heights, it is more useful to plot meteors on a speed/begin height graph, since this makes the dependence of begin height on speed clear. Ideally, the zenith angle would also be included, but the effect of the zenith angle on the initial height is much less than the effect of the speed.

Of the 5092 meteors observed by the influx system, we removed those which did not both begin and end in the field of view, those with a convergence angle (angle between the planes formed by the meteor's path and each of the cameras) less than 5°, meteors for which orbits could not be determined, and meteors with very few points. This left 3491 high quality meteors. For the mirror system, of the 4052 two-station meteors, 3521 passed the same filters. The higher fraction of useful meteors in the mirror system reflects the lack of detection of faint meteors for this system, meaning those meteors which are recorded have longer trails and better signal-to-noise.

Fig. 1 shows density plots of begin heights versus speed for the influx and tracking systems. Both show the same trend of increasing begin height with speed, and a rough division into two populations: a (presumably weaker or more volatile) higher population and a (presumably stronger or more refractory) lower population. These two populations cover the full range of speeds.

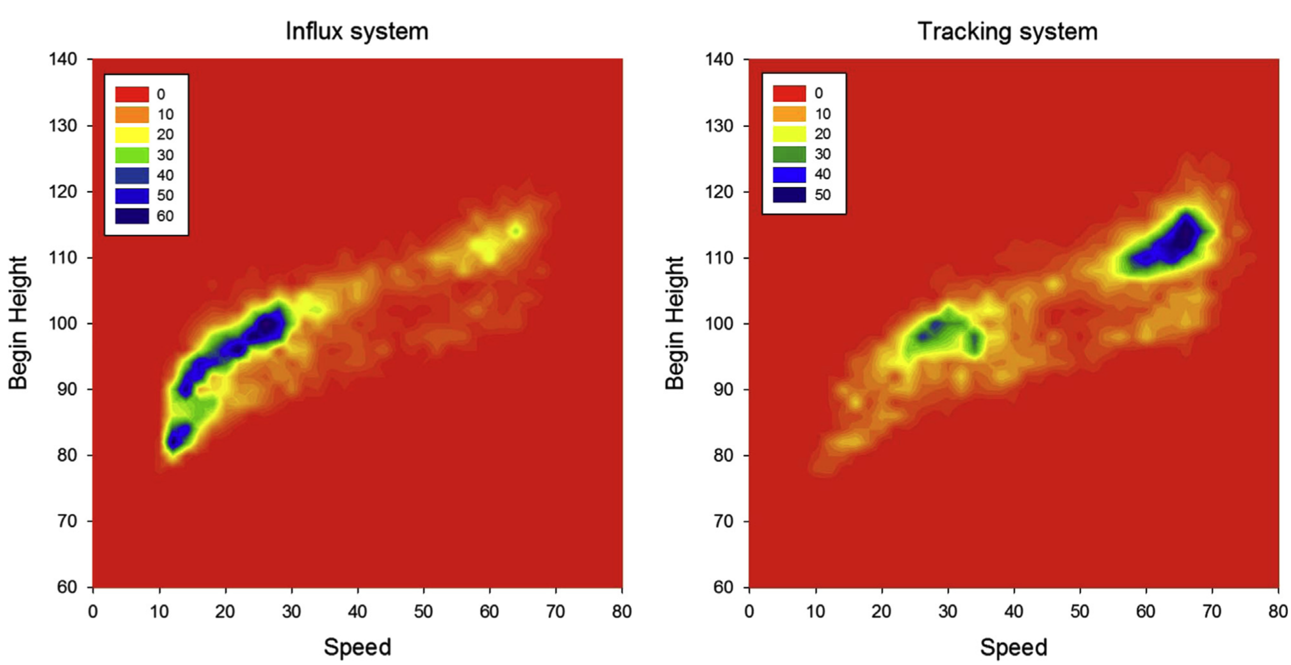

Fig. 1. Begin height and speed distributions for the influx system (left) and tracking system (right).